the negative charge carriers (sulfonate groups) cannot easily approach the pyrrole ring site to form ring–anion pairs which are suitable for specific electrostatic interaction. The specific anion–ring electrostatic interaction is replaced by uniform charge extraction from the polymer backbone in the latter case. Our data indicate that when the negative charge carriers are not located in close proximity to the pyrrole ring site, the charge is withdrawn from the π-conjugated carbon path, and the created cation hole is delocalized and does not affect the nitrogen heteroatom.

Registry No. $PPy^+ClO_4^-$, 82200-25-7; PVS, 26101-52-0; PSS, 50851-57-5; PPy, 30604-81-0.

Time-Resolved in Situ X-ray Difffraction Studies of a Lithium Nickel Oxide Catalyst during the Oxidative Coupling of Methane

Ingrid J. Pickering,*[1] Peter J. Maddox,[2] and John M. Thomas*

Davy Faraday Research Laboratory, The Royal Institution of Great Britain, 21 Albermarle Street, London W1X 4BS, U.K.

Received December 10, 1991. Revised Manuscript Received June 4, 1992

A lithium nickel oxide catalyst of composition $Li^+_xNi^{2+}_{1-2x}Ni^{3+}_xO$, $x = 0.45$, active in the oxidative coupling of methane, has been studied in the presence and absence of added gaseous oxygen at 700 °C using simultaneous in situ X-ray powder diffraction with gas chromatography. In the presence of gaseous oxygen the bulk structure remains essentially unchanged for more than 5 h, and during this time the catalyst is selective for C_2 production; following this there is rapid reduction of the catalyst through NiO to Ni metal, with corresponding evolution of CO_2 and finally CO as the dominant gaseous products. By contrast, in the absence of gaseous oxygen the bulk structure immediately starts to decompose, yielding successively a total of four rock salt-type lithium nickel oxide phases. In this case the initial selectivity for C_2 production is 100% and declines as the solid breaks down. The in situ measurements allow direct correlation of the appearance of different solid phases during the experiments with variations in the rate of production of gaseous products, giving important insights into the behavior of this material as catalyst. A reaction scheme is proposed based on the catalytic and structural results. Additional studies of the structure of $Li^+_{0.45}Ni^{2+}_{0.10}Ni^{3+}_{0.45}O$ as a function of temperature in air using Rietveld structure refinements have been carried out to augment the in situ studies, showing that the ordered lithium nickel oxide structure is essentially invariant up to 700 °C in air.

Introduction

There has been much interest in the conversion of methane, an abundant natural resource, to more economically useful products by direct oxidation using heterogeneous catalysis. Although some attention has been given to the oxidation of methane to methanol and formaldehyde,[3] the majority of the research has involved the oxidative coupling of methane to ethane and ethene.[4] The oxide catalysts used have involved a wide variety of cations, including those from the s and p block, especially Li/MgO,[5] the lanthanides, notably Sm_2O_3,[6] transition metals,[7] and complex compounds, including oxychlorides.[8] Lithium-doped solids have received much attention as catalysts for oxidative coupling, particularly Li^+/MgO.[9]

Various alkali-metal-doped first-row transition-metal oxides have been screened by Hatano and Otsuka for their selectivity toward methane coupling,[10] and they concluded that lithium-doped nickel oxide was the most promising catalyst. Ungar et al.[11] have investigated various complex oxides with rock salt structures; the two most promising catalysts included in their study, $LiNiO_2$ and $LiYO_2$, have different structures and apparent mechanisms for oxidation. $LiNiO_2$ appeared to involve a bulk redox mechanism (in agreement with Hatano and Otsuka[10]), whereas $LiYO_2$ apparently catalyzed the oxidation of methane via a surface reaction. In further studies of the lithium nickel oxide catalyst, Hatano and Otsuka have shown[10] that an increase of lithium in the catalyst increases the selectivity for C_2 hydrocarbons, and they have used temperature-programmed desorption measurements to show that oxygen is desorbed in vacuo above 873 K, with a peak at ca. 1100 K. They have additionally investigated[12] the effect of changing pressures of reactants, C_2 selectivity increasing

(1) Currently at Stanford Synchrotron Radiation Laboratory, P.O. Box 4349, Bin 69, Stanford, CA 94309-0210.
(2) Currently at BP Research International, Sunbury Research Centre, Chertsey Road, Sunbury-on-Thames, Middlesex TW16 7LN, U.K.
(3) Pitchai, R.; Klier, K. *Catal. Rev.-Sci. Eng.* **1986**, *28*, 13.
(4) Hutchings, G. J.; Scurrell, M. S.; Woodhouse, J. R. *Chem. Soc. Rev.* **1989**, *18*, 251.
(5) Ito, T.; Lunsford, J. H. *Nature* **1985**, *314*, 721.
(6) Otsuka, K.; Jinno, K.; Morikawa, A. *J. Catal.* **1986**, *100*, 353.
(7) Burth, R.; Squire, G. D.; Tsang, S. C. *Appl. Cat.* **1988**, *43*, 105.
(8) Ueda, W.; Thomas, J. M. *J. Chem. Soc., Chem. Commun.* **1988**, 1148.
(9) Ito, T.; Wang, J.-X.; Lin, C.-H.; Lunsford, J. H. *J. Am. Chem. Soc.* **1985**, *107*, 5062.
(10) Hatano, M.; Otsuka, K. *Inorg. Chim. Acta* **1988**, *146*, 243.
(11) Ungar, R. K.; Zhang, X.; Lambert, R. M. *Appl. Catal.* **1988**, *42*, L1.
(12) Hatano, M.; Otsuka, K. *J. Chem. Soc., Faraday Trans. 1* **1989**, *85*, 199.

0897-4756/92/2804-0994$03.00/0

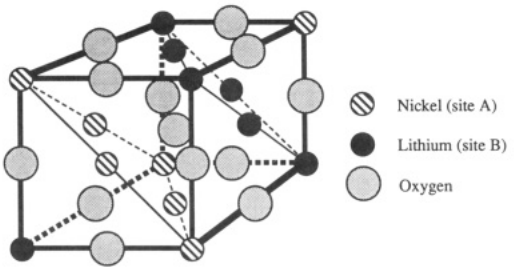

Figure 1. Idealized structure of $Li^+_xNi^{2+}_{1-2x}Ni^{3+}_xO$ for $x = 0.5$.

sharply with increasing methane pressure, and CO_2 production being enhanced by increased oxygen pressure. C_2 selectivity additionally increases with temperature.

Lithium nickel oxides, $Li^+_xNi^{2+}_{1-2x}Ni^{3+}_xO$, $0 \le x \le 0.5$, are all related to the face-centered cubic rock salt structure.[13,14] At room temperature in pure NiO there is a very slight rhombohedral distortion associated with magnetic order,[15] which disappears above 250 °C. For low lithium loadings, approximately in the range $0 < x \le 0.25$, Li^+ forms a random substitutional solid solution with nickel. The addition of lithium causes the lattice to contract in a monotonic fashion, due to the oxidation of Ni^{2+} to Ni^{3+} with the resulting decrease in cation size; the Li^+ cation is itself similar or slightly larger in size compared with the Ni^{2+} cation.[16] For higher values of x a phase "$LiNiO_2$"[17] is formed which has a degree of ordering of the lithium and nickel on every other close-packed (111) layer and a rhombohedral unit cell ($R\bar{3}m$). An idealized structure for $x = 0.5$ is shown in Figure 1. There is a small rhombohedral distortion of the structure away from true cubic close packing (<1% for all cases). The increasing intensity of superlattice lines shows that ordering between the close-packed layers increases for x in this compositional region.

The aim of the present paper is to investigate the correlation between the bulk structure and the catalytic properties of $Li^+_xNi^{2+}_{1-2x}Ni^{3+}_xO$ using in situ X-ray powder diffraction results. Studies are presented of both catalytic and stoichiometric systems (in the presence and absence of added gaseous oxygen). The reaction scheme is discussed in the light of these and previous results. A short communication on the in situ study of the catalytic oxidative coupling of methane using powder diffraction has been previously published.[18]

Experimental Section

Lithium nickel oxides, $Li^+_xNi^{2+}_{1-2x}Ni^{3+}_xO$ ($0 < x \le 0.5$) were prepared by a solid-state reaction of Li_2CO_3 and NiO in stoichiometric proportions. The amounts were ground intimately and placed in an alumina crucible and then fired at 800 °C in air. Typically rates were 10 °C min^{-1} while heating and 2 °C min^{-1} during cooling. The sample was removed and ground, a diffraction pattern was taken, and the sample was then replaced in the furnace for a further heating cycle. This process was repeated until the diffraction pattern showed no trace of Li_2CO_3 and the lattice parameters of the product phase did not decrease with further heating. The ratio of lithium to nickel in the sample was determined by atomic absorption spectroscopy and was in good agreement with the starting ratios in the reactant mixture.

Table I. Conditions Used for the in Situ Reactions of Lithium Nickel Oxide with Methane[a]

experiment	mass, g	gas composition, % CH_4	O_2	N_2	XRD dwell time per step, s
stoichiometric	1.04	20	0	80	0.5
catalytic	1.01	20	3	77	1

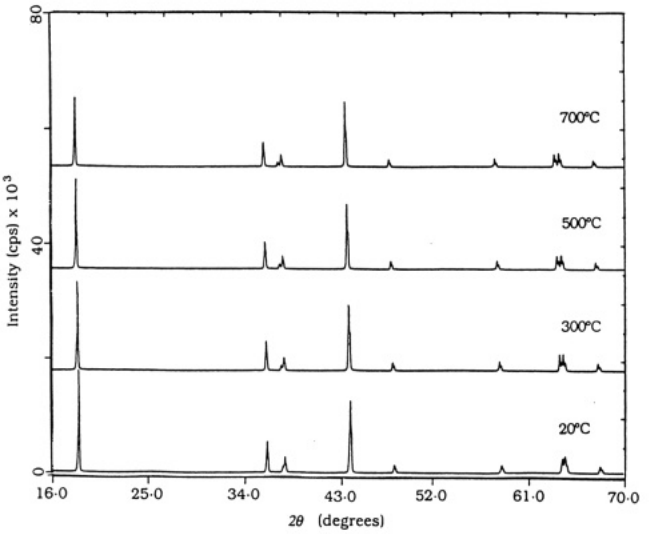

Figure 2. Powder X-ray diffraction patterns recorded using Cu Kα radiation while heating $Li^+_xNi^{2+}_{1-2x}Ni^{3+}_xO$, $x = 0.46$, in air. The temperatures for each pattern are shown. Data were collected with a step size of 0.02° 2θ.

Powder X-ray diffraction patterns were collected using Cu Kα radiation by means of a Siemens D500 diffractometer equipped with a Stöe rotating anode source operating at 12 kW. Diffraction patterns at elevated temperatures in air were collected for a sample with $x = 0.46$. The sample was mounted in a pyrophyllite block wound internally with nichrome wire as a heater. Temperature was measured by means of a thermocouple placed in a machined hole in the block in close proximity to the sample. Diffraction patterns were taken at 20, 300, 500, and 700 °C in air.

Rietveld profile refinements[19] using the X-ray diffraction patterns were carried out using Larson and von Dreele's generalized crystal structure analysis system (GSAS).[20] The model assumes a rhombohedral unit cell ($R\bar{3}m$, No. 166) using the hexagonal setting. There are two cation sites, A at site 3a (0,0,0) and B at 3b (0,0,$^1/_2$), with the oxygen at 6c (0,0,z), $z = 0.25$. The starting model confined the lithium to site B with site A exclusively nickel. A constraint was applied so that the overall lithium-to-nickel ratio was invariant (0.46) and cation site occupancies were varied as a single parameter. X-ray scattering factors used were for O^-, Li^+, and Ni^{3+}. Anomalous dispersion corrections were applied for Ni at the wavelength of Cu Kα. The temperature parameters for all atoms were constrained to be equal. A pseudo-Voigt profile function was assumed, with five refined coefficients. The model was refined until profile and structural parameters converged.

In situ gas–solid reactions, both stoichiometric and catalytic, were carried out at 700 °C using a specially designed in situ reactor which is described elsewhere.[21] This allows simultaneous monitoring of both the structure of the solid, by powder diffraction, and the appearance of gaseous products, using gas chromatography. The cell was attached to the rotating anode system as described above. A Perkin-Elmer gas chromatograph was used with a Carbosieve G column and a flame-ionization detector fitted with a catalytic converter to reduce CO and CO_2 to CH_4 before

(13) Goodenough, J. B.; Wickham, D. G.; Croft, W. J. *J. Phys. Chem. Solids* **1958**, *5*, 107.
(14) Li, W.; Reimers, J. N.; Dahn, J. R. *Phys. Rev. B*, submitted 1991.
(15) Bartel, L. C.; Morosin, B. *Phys. Rev. B* **1971**, *3*, 1039.
(16) Deren, J.; Rekas, M. *Pol. J. Chem.* **1972**, *46*, 1411.
(17) Dyer, L. D.; Borie, B. S., Jr.; Smith, G. P. *J. Am. Chem. Soc.* **1954**, *76*, 1499.
(18) Pickering, I. J.; Maddox, P. J.; Thomas, J. M. *Angew. Chem., Int. Ed. Engl. Adv.: Mater.* **1989**, *28*, 808.
(19) Rietveld, H. M. *J. Appl. Crystallogr.* **1969**, *2*, 65.
(20) Larson, A. C.; von Dreele, R. B. *Generalized Crystal Structure Analysis System*; Los Alamos National Laboratory, Los Alamos, NM.
(21) Pickering, I. J.; Madill, D.; Sheehy, M.; Stachurski, J. M.; Maddox, P. J.; Couves, J. W.; Dooryhee, E.; Thomas, J. M. *J. Chem. Soc., Faraday Trans.* **1991**, *87*, 3063.

Table II. Refinement Details for X-ray Powder Diffraction Refinements of Lithium Nickel Oxide Located in Air[a]

	20 °C	300 °C	500 °C	700 °C
R_{wp}	3.73	3.12	2.97	3.35
R_p	2.55	2.22	2.21	2.44
reduced χ^2	2.1386	1.7287	1.6075	1.7607
a_o (Å)	2.8853 (1)	2.8927 (1)	2.8993 (1)	2.9053 (1)
c_o (Å)	14.2162 (10)	14.2745 (6)	14.3242 (6)	14.3653 (7)
zero-point correction (°2θ)	0.0126 (9)	−0.0004 (6)	−0.0110 (6)	−0.0269 (7)
U_{iso}	0.0045 (8)	0.0016 (7)	0.0020 (7)	0.0012 (8)
oxygen z coordinate	0.2582 (2)	0.2586 (2)	0.2589 (2)	0.2585 (2)
site occupancies				
Ni on site A	0.992 (2)	1.000 (2)	1.005 (2)	1.002 (2)
Ni on site B	0.088 (2)	0.080 (2)	0.075 (2)	0.078 (2)
Li on site A	0.008 (2)	0.000 (2)	−0.005 (2)	−0.002 (2)
Li on site B	0.912 (2)	0.920 (2)	0.925 (2)	0.922 (2)
profile parameters				
U	−48 (13)	10 (6)	−10 (5)	30 (6)
V	73 (9)	30 (4)	23 (4)	−15 (5)
W	−4.0 (13)	6.8 (8)	2.1 (9)	9.6 (9)
X	0.8 (2)	1.4 (2)	1.6 (2)	1.3 (2)
Y	8.0 (9)	5.3 (6)	4.5 (6)	5.3 (7)
A_s	4.65 (4)	3.91 (4)	4.05 (3)	3.80 (4)
bond length, Å				
A–O	1.979 (5)	1.982 (5)	1.985 (4)	1.992 (5)
B–O	2.113 (5)	2.124 (5)	2.132 (4)	2.134 (4)
A–A	2.885 (2)	2.893 (1)	2.899 (1)	2.905 (1)
A–B	2.896 (5)	2.907 (4)	2.916 (4)	2.923 (5)
O–O (×3)	2.710 (7)	2.710 (6)	2.711 (6)	2.726 (5)
O–O (×6)	2.885 (2)	2.893 (1)	2.899 (1)	2.905 (1)
O–O (×3)	3.089 (8)	3.110 (6)	3.128 (5)	3.128 (7)

[a] $Li_xNi_{1-x}O$; $x = 0.46$. Reduced $\chi^2 = M/(N_{obs} - N_{var})$ and $R_{wp} = [M/\sum(wI_o^2)]^{1/2}$ where the quantity minimized is $M = \sum w(I_o - I_c)$, with I_o I_c being the observed and calculated intensities and w a weight related to the error. N_{obs}, the number of observations is 2701 and N_{var}, the number of variables, is 16 for each refinement. U_{iso} are expressed as the square atomic displacement in Å. A cosine Fourier series was used as a background function with three refined coefficients. A pseudo-Voigt profile function was used with the Gaussian variance equal to $U \tan^2\theta + V \tan\theta + W$ and the Lorentzian coefficient as $X/\cos\theta + \tan\theta$. The asymmetry term A_s modifies the peak shape by a term $A_s/\tan 2\theta$. See ref *19* for details.

detection. The sample used was a high-lithium content lithium nickel oxide with $x = 0.45 \pm 0.02$. Two complementary experiments were carried out; in the first, a mixture of methane and nitrogen only was passed over the catalyst at temperature, and in the second gaseous oxygen was added to the feed. Conditions for the in situ experiments are shown in Table I.

Results

Rietveld Profile Refinements at Elevated Temperatures. As a preliminary to the catalytic studies, the behavior of the catalyst was investigated as a function of temperature in air. The diffraction patterns collected at elevated temperatures in air are shown in Figure 2. The rhombohedral phase of lithium nickel oxide is the only phase present throughout the temperatures investigated (20–700 °C). Rietveld profile refinements were carried out using each of the data sets, and the results of the refinements are given in Table II. The unit cell parameters vary smoothly with temperature. The linear coefficients of expansion as deduced from the lattice parameters after refinement are 1.03×10^{-5} and 1.56×10^{-5} K^{-1} for a and c, respectively. The refinements give the occupancy of lithium on the minority sites (site A) to be 0.00 ± 0.01, showing that the structure is fully ordered at all temperatures studied. Linear expansion coefficients for the M–O bonds are calculated to be 0.88×10^{-5} K^{-1} and 1.50×10^{-5} K^{-1} for bonds A–O and B–O, respectively.

The refinements demonstrate that on heating to the reaction temperature in air alone the structure of the catalyst is invariant. The room-temperature results are in excellent agreement with those of Morales et al.,[22] who

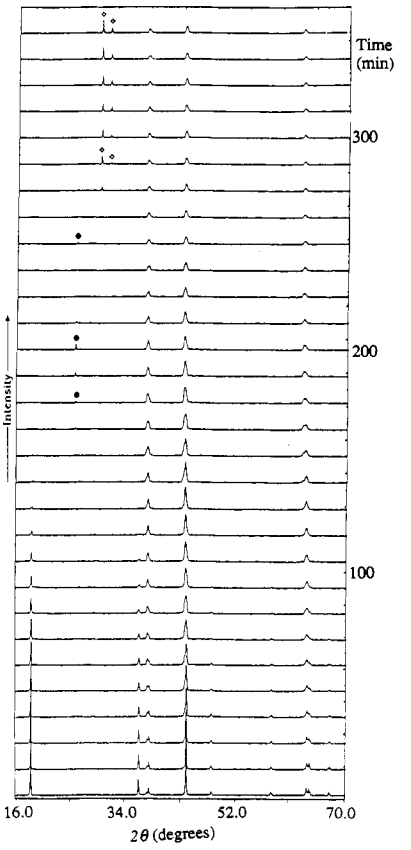

Figure 3. Diffraction patterns recorded in situ during the stoichiometric reaction of methane with lithium nickel oxide. Time of reaction is shown on the right. The initial phase is rhombohedral lithium nickel oxide. Peaks are labeled as follows: ● Li_2NiO_2, ◇ Li_2CO_3.

(22) Morales, J. P.; Pérez-Vicente, C.; Tirado, J. L. *Mater. Res. Bull.* **1990**, *25*, 623.

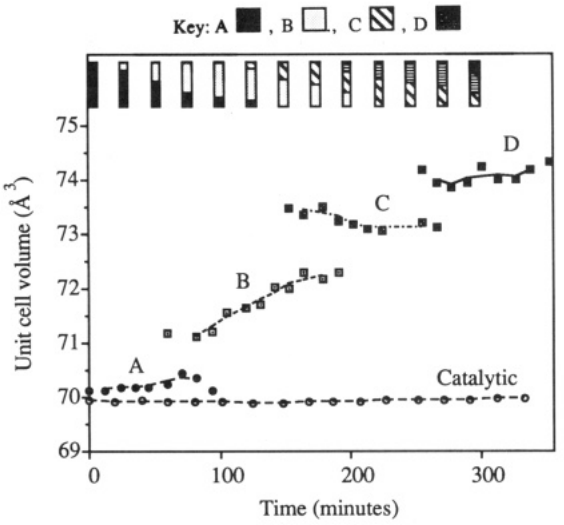

Figure 4. Variation of unit cell volume with time for the rocksalt lithium nickel oxide phases during the course of the stoichiometric reaction (labeled A–D) and the catalytic reaction. Unit-cell volumes are expressed as the volume of 4 lattice motifs, i.e., two-thirds of the rhombohedral unit cell (using the hexagonal setting) for the ordered "$LiNiO_2$"-type structure and one face-centred cubic unit cell in the case of the random solid solution. The histograms at the top of the diagram represent the observed fractional distribution of phases during the stoichiometric reaction as a function of the same time axis. The fractions are estimated by fitting the strongest diffraction peaks (ca. 44° 2θ) with a set of pseudo-Voigt peak functions.

carried out a structural refinement on a sample with x = 0.46.

In Situ Stoichiometric Reaction. The diffraction patterns for the stoichiometric reaction (20% CH_4 in N_2, no added O_2) are shown in Figure 3 as a function of time at 700 °C. They exhibit gradual change with time. The peaks of the initial, ordered phase decrease in intensity with time, as can be seen particularly for the superlattice peaks at $2\theta \approx 18°$ and 36°. At the same time, new peaks appear close to the low-angle side of the sublattice peaks, indicating that the reactant phase is decomposing to give other rock salt-type phases which do not have cation ordering. Detailed analysis of the time-resolved diffraction patterns identifies three such disordered phases appearing during the decomposition.

Lattice parameter refinements were carried out to determine the unit cell volume of each phase as the sample is reduced by methane, and the results are plotted in Figure 4 as a function of time. The original phase (A) was indexed as a rhombohedral unit cell, and subsequent ones (labeled B–D) as a cubic unit cell (random solid solution). The increase in volume indicates a gradual loss of lithium from the $Li_xNi_{1-x}O$ phases as oxygen is removed. The discontinuities in the values of volume observed suggests that there may be discrete values of x occurring in the $Li_xNi_{1-x}O$ phases under these conditions.

Up until ~160 min, the only diffraction peaks appearing are due to the $Li_xNi_{1-x}O$ rock salt structures. After this time another phase starts to appear, with its strongest peak at $2\theta \approx 25.7°$ (see Figure 3), which is due to Li_2NiO_2.[23] Near the end of the experiment there also appear two peaks at 29.6° and 31.0°, which are sharp and grow with time. These peaks may be assumed to belong to a highly orientated form of lithium carbonate, since on cooling to room temperature the peaks are at the correct angles for Li_2CO_3 and after removing the sample from the reactor and

(23) Rieck, H.; Hoppe, R. *Z. Anorg. Allg. Chem.* **1972**, *392*, 193.

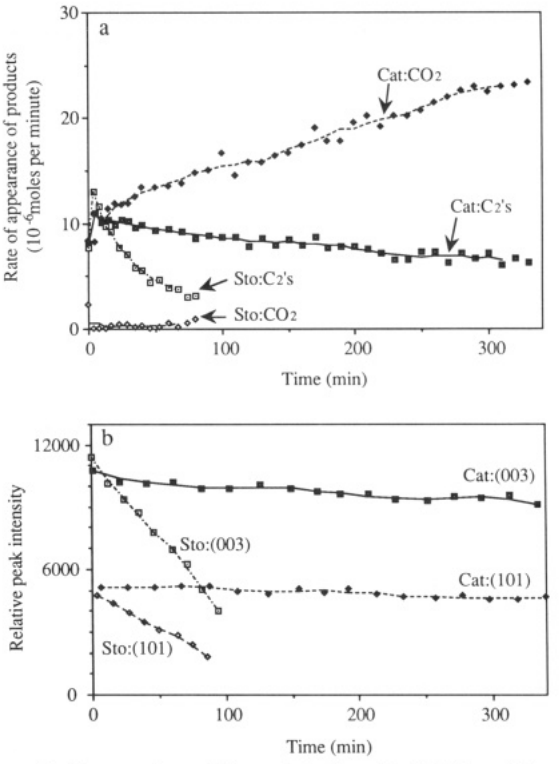

Figure 5. Comparison of the catalytic and stoichiometric reactions: (a) Rate of appearance of products with time. Cat, catalytic; Sto, stoichiometric. CO_2, rate of appearance of CO_2 with time; C_2's, rate of appearance of (C_2H_6 + C_2H_4) with time. Note the similarity of the C_2 rates at the beginning and the dissimilarity of those of CO_2. (b) Variation in the intensities of two of the superlattice peaks. C, catalytic; S, stoichiometric. Indexes refer to the peaks used: (003) ≈ 18°, (101) ≈ 36° 2θ.

mixing, the diffraction pattern unambiguously shows Li_2CO_3 (other phases were Li_2NiO_2 and a rock salt phase with very low x).

The rates of appearance of gaseous products as determined by gas chromatography during the in situ reaction are shown in Figure 5a. The carbon-containing gaseous products for the stoichiometric reaction are ethane, ethene, and carbon dioxide. At the start of the experiment CO_2 production is very slow, and C_2 hydrocarbons are formed with apparent 100% selectivity assuming little CO_2 hold up on the catalyst. Clearly the structural oxygen from the ordered $Li_xNi_{1-x}O$, the oxidant in this reaction, is highly selective for methane coupling. The rate of methane conversion decays during the first 100 min due to the depletion of the structural oxygen. CO_2 is also formed in increasing proportion with time and is the dominant gaseous species produced in the later stages of the reaction (although at this time total rates are small). The decay of the C_2 production (Figure 5a) is correlated with the removal of the original, ordered rock salt phase, which is represented in Figure 5b by a plot of the intensity of two superlattice peaks as a function of time. The ordered phase is replaced by a disordered phase which has a significant lithium fraction as judged by its unit-cell volume. However, this latter phase produces largely CO_2, suggesting that the ordering of the cation layers may be significant with respect to the ability of the oxide to produce ethane and ethene.

In Situ Catalysis. The in situ diffraction patterns for the catalytic reaction at 700 °C (20% CH_4, 3% O_2, balance N_2) are shown in Figure 6 as a function of time. In direct contrast to the stoichiometric reaction, the bulk structure remains constant for several hours and then exhibits a sudden change. For the first 330 min, there is essentially

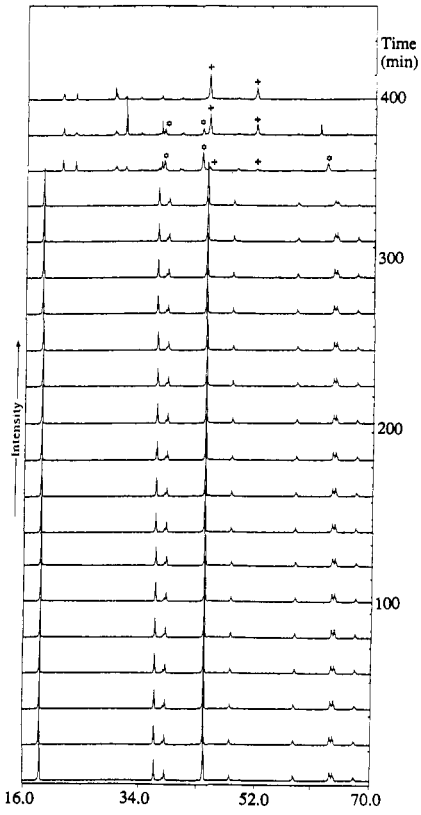

Figure 6. Diffraction patterns recorded in situ during the catalytic reaction of methane with lithium nickel oxide. Time of reaction is shown on the right. The initial phase is rhombohedral lithium nickel oxide. Dramatic change occurs after ~330 min. Peaks are labelled as follows: o NiO, + Ni metal. The remaining peaks in the final three patterns may be due to lithium carbonate.

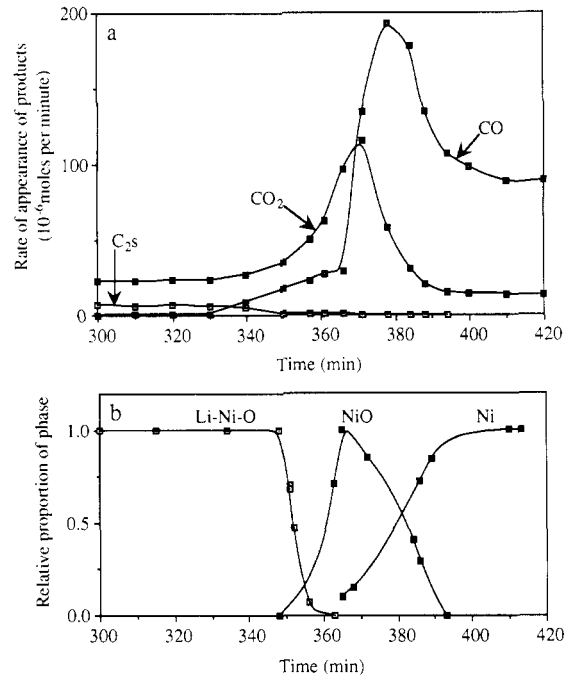

Figure 7. Comparison of the rate of appearance of gaseous products (a) with the changes in proportions of phases (b) as they change with time for the in situ catalytic reaction. Phase proportions are estimated from the intensities of individual peaks in the diffraction pattern. The decay of the starting material, Li–Ni–O, is normalized to the intensity of the same peaks in earlier patterns. Ni metal peaks are normalized to the intensities in the final high-temperature pattern. NiO peaks are estimated from the observed ratio of peak intensities (111):(200):(220) as 0.69:1.00:0.57 and normalized to the maximum observed value.

no change in the Li–Ni–O diffraction pattern, with no appearance of any other phase. The unit cell volume, plotted in Figure 4, is constant with time, and the intensities of the superlattice peaks, shown in Figure 5b, show little change. The rates of appearance of C_2(s) and CO_2 during this initial period (Figure 5a) show that the rate of C_2 production is decreasing slightly during this time and the rate of CO_2 production is increasing. These values correspond to a near constant methane conversion of ca. 8% and an initial C_2 selectivity of around 68%, decreasing to ca. 33% at t = 330 min.[24] The ratio of C_2H_4/C_2H_6 is also steady at around 0.35 during this time.

At about 340 min the diffraction patterns exhibit a dramatic change, with the $Li_xNi_{1-x}O$ decomposing to give NiO. Figure 7 shows a comparison of the changes in composition of the gaseous and solid phases. There is a maximum in CO_2 production at 370 min which coincides with the maximum in the NiO at 366 min as determined by diffraction peak intensity. This suggests that NiO is briefly acting as a deep oxidation catalyst at this time (NiO is a known deep oxidation catalyst.[25]) The system then changes further, with NiO being reduced to Ni metal, and at the same time CO replacing CO_2 as the dominant product in the gas phase. This indicates that at this final stage Ni metal is the catalyst facilitating the oxidation of CH_4 to CO, and H_2 is the probable hydrogen-containing product.

Table III. Summary of the Phases Appearing and Corresponding Reactions Catalyzed during the in Situ Catalysis Experiment of Methane with $Li_xNi_{1-x}O$. The Major Phases Listed Are Those Containing Nickel

time, min	major phase	reaction catalyzed
$0 < t \lesssim 330$	$Li_xNi_{1-x}O$	$2CH_4 + {}^1/_2O_2 \rightarrow C_2H_6 + H_2O$ $CH_4 + 2O_2 \rightarrow CO_2 + 2H_2O$
$330 \lesssim t \lesssim 380$	NiO	$CH_4 + 2O_2 \rightarrow CO_2 + 2H_2O$
$t \gtrsim 380$	Ni metal	$CH_4 + {}^1/_2O_2 \rightarrow CO + 2H_2$

In addition to NiO and Ni, other peaks are observed in the diffraction patterns at 700 °C in the latter stages of the reaction which are more difficult to assign (see Figure 6). The intensities of the extra peaks change with time in a nonsystematic way possibility due to local exotherms which raise the temperature of the sample above the melting point of Li_2CO_3 (723 °C[26]). On cooling to room temperature, at the end of the experiment peaks due to lithium carbonate are unequivocally observed.

The major phases appearing and the dominant reactions catalyzed are summarized in Table III.

Discussion

Our results show that, with a cofeed of methane, oxygen, and nitrogen, the ordered phase of lithium nickel oxide was unchanged during an initial period which corresponded to the catalyst selectively producing ethane and ethene. After this period of some 5 h, the catalyst was suddenly reduced, first to nickel oxide and then to nickel metal. The final dominant gaseous product after catalyst reduction was carbon monoxide, and the catalyst reduction as observed

(24) Percentage conversion of methane (C) and selectivity for C_2 hydrocarbons (S) are defined as follows: $C = 100\,\Sigma^n V_{C_n}/(V_{CH_4}+\Sigma^n V_{C_n})$; and $S = 100(2V_{C_2H_6} + 2V_{C_2H_4})/\Sigma^n V_{C_n}$.

(25) Otsuka, K.; Liu, Q.; Morikawa, A. *Inorg. Chim. Acta* **1986**, *118*, L23.

(26) *Handbook of Chemistry and Physics*, 69th ed.; Weast, R. C., Ed.; CRC Press: Boca Raton, FL; 1988–89.

by XRD corresponded very precisely with the changes in the gaseous product distributions. When methane and nitrogen were supplied to the oxide in the absence of gaseous oxygen, the bulk decomposition as monitored by XRD commenced immediately and was smooth as a function of time. A total of four rock salt phases were identified during the course of this stoichiometric reaction; the initial, ordered phase was replaced, as the reaction progressed, with random solid solutions of lithium in nickel oxide, the phases having successively smaller lithium loadings. At the onset of reaction, C_2 hydrocarbons were the only carbon-containing gaseous products detected, although as the reaction progressed their rate of production decayed, and they were replaced by CO_2 as the carbon-containing product. Rietveld profile analysis of the catalyst phase at elevated temperature in air showed that, apart from thermal expansion, there was no change in the catalyst due to the thermal treatment alone.

The combined in situ results from both the catalytic and the stoichiometric reactions demonstrate that the presence of the bulk, ordered lithium nickel oxide phase is crucial for the production of the C_2 hydrocarbons. In the former reaction, C_2's are produced for some 330 min, coincident with bulk lithium nickel oxide being present as deduced by XRD. In the latter reaction, C_2 hydrocarbons are produced only at the start of the reaction, before the ordered phase is decomposed. Both reactions point to the presence of bulk lithium nickel oxide as facilitating the selective oxidation. Furthermore, a comparison of the initial rates of C_2 production during the stoichiometric and catalytic reactions shows that the rates are very similar irrespective of the presence of gaseous oxygen in the gas stream. This suggests that in both cases it is the same species which is responsible for the production of C_2 hydrocarbons, and this species may be either a surface chemisorbed or activated metal oxide.

In the case of the production of CO_2, a comparison of the catalytic and stoichiometric reactions shows that while this species is produced in significant quantities in the presence of gaseous oxygen, it is essentially absent during the initial stages of the stoichiometric reaction when there was no added gaseous oxygen. These observations suggest that the production of CO_2 involves either a surface or gaseous oxygen species. One possible explanation is that the CO_2 is produced by interaction of the gaseous oxygen with a surface-generated gaseous methyl radical. These observations are in agreement with those of Hatano and Otsuka,[10,12] who also suggest that there are two distinct types of oxygen involved, just as there are in other selective oxidations of hydrocarbons.[27]

Hatano and Otsuka have proposed[12] a reaction scheme involving dissociative adsorption of the methane on surface Ni^{3+}–O^{2-} sites, followed by coupling of the CH_3 groups to form C_2H_6 and loss of water. They also propose that the overall mechanism involves the breakdown of the lithium nickel oxide to form nickel oxide and lithium oxide, with gaseous oxygen then regenerating the original lithium nickel oxide. From our in situ results, there is no evidence for the formation of bulk NiO during the catalytic process. However, since XRD is a bulk, rather than a surface technique, our results do not preclude the possibility that the surface is indeed broken down into the constituent oxides, dispersion control being maintained by the underlying solid solution. We can also, however, envisage another scheme in which oxygen, consumed in the oxidative coupling of methane, is removed from the lithium nickel oxide structure to give a compound $Li_xNi_{1-x}O_{1-\delta}$, having a small deficit of oxygen. In the catalytic reaction gaseous oxygen can replenish this deficit and stabilize the solid, whereas in the stoichiometric reaction, as oxygen is withdrawn the solid rapidly achieves too large an anion deficit and decomposes to give another rock salt phase of lower lithium content.

The abrupt change in catalyst and gaseous compositions during the catalytic reaction after apparent stability for several hours can be attributed to the gradual change in gaseous product composition. The rate of CH_4 conversion changes little, but there is an increase in CO_2 at the expense of C_2 hydrocarbons. This substantially affects the rate of consumption of oxygen, which begins at around 50% and rises to close to 100% by 330 min. When all the supplied gaseous oxygen is being consumed, the atmosphere suddenly becomes reducing and bulk decomposition of the catalyst ensues. Once started, the decomposition is much more rapid than in the stoichiometric case due to the large proportion of CO_2 in the gas phase, which drives the solid products toward lithium carbonate. Finally, CO is also formed as a gaseous product and in the highly reducing conditions NiO is rapidly reduced to metallic nickel. The time of decomposition of the catalyst therefore depends critically on the partial pressure of oxygen in the system. Independent results have shown[28] that a higher partial pressure of oxygen does indeed prolong the selective regime of the catalyst before its reduction. However, such an atmosphere also generates a greater proportion of CO_2, thereby reducing the selectivity of the system for C_2 hydrocarbon species.

Summary

Our results illustrate the merit of combining quantitative, in situ X-ray powder diffractometry with gas-chromatographic monitoring of changes in gas-phase composition during the course of both stoichiometric and catalytic processes involving the oxidative coupling of methane over the oxide $Li^+_{0.45}Ni^{2+}_{0.10}Ni^{3+}_{0.45}O$. Powerful insights into the nature and degree of cation ordering of various solid phases were obtained and it proved possible to identify which particular solid phase was associated with an observed change in gas composition.

Acknowledgment. We thank Prof. A. K. Cheetham for helpful discussions during the course of this work and also Prof. A. J. Jacobson for his advice and assistance. We are grateful to the Science and Engineering Research Council for a rolling grant (to J.M.T.), a fellowship to (P. J. M.) and a studentship (to I.J.P.)

Registry No. $Li^+_{0.45}Ni^{2+}_{0.10}Ni^{3+}_{0.45}O$, 142395-58-2; methane, 74-82-8; oxygen, 7782-44-7.

(27) Kaliberdo, L. M.; Tselyutuia, M. I.; Vaabel, A. S.; Kalikhman, V. M.; Shvetsov, B. N. *Russ. J. Phys. Chem.* **1979**, *53*, 843.

(28) Lewandowski, J. T.; Jacobson, A. J.; Hall, R. B., private communication.